Journal of Simulation and Analysis of Novel Technologies in Mechanical Engineering 17 (2) (2025) 0005~0020 DOI 10.71939/jsme.2025.1208905

Research article

Numerical study of a self-adjusting blade turbine: model validation and parametric analysis

Fatemeh Behrouzi^{1*}, Adi Maimun bin Abdel Malikb², Yasser M. Ahmed³

¹Department of Mechanical Engineering, Bu.C., Islamic Azad University, Bushehr, Iran ²Marine Technology Centre, Universiti Teknologi Malaysia (UTM), 81310 Skudai, Johor, Malaysia ³Faculty of Engineering, Alexandria University, Egypt

* Fatemeh.Behrouzi@iau.ac.ir and Fatemeh.behrouzi2012@gmail.com

(Manuscript Received --- 04 June 20025; Revised --- 30 July 2025; Accepted --- 11 Aug. 2025)

Abstract

The plentiful advantages of the vertical axis turbine, have caused significant growth in vertical axis turbine research and development. This research paper presents a numerical study of self-adjusting blades turbine, as an alternative to the Savonius-based turbine. Unsteady Reynolds-averaged Navier–Stokes equations with the Semi-Implicit Method for Pressure-Linked Equation algorithm and a k- ω Shear Stress Transport turbulence model have been applied in computational fluid dynamics simulations. The dynamic behavior of fixed and self-adjusting blade turbines has been simulated numerically at a low flow speed of 0.32 m/s. The rotational motions of fixed and self-adjusting blade turbines were solved using the sliding mesh model and dynamic mesh motion, respectively. Additionally, the results of performance analysis were validated by the experimental data. The performance and flow characteristics of the self-adjusting blades turbine for different arm length to bucket diameter ratios (r/d) and blade angles (β) were discussed and analyzed. Moreover, C_Pmax and tip speed ratio for the modified turbine were found for flow velocities from 0.17 m/s to 0.64 m/s. the maximum performance of the modified self-adjusting blades turbine was 0.16 at tip speed ratio, λ =0.45 which the torque coefficient corresponding to maximum power coefficient was 0.34.

Keywords: Novel vertical axis turbine, Self-Adjusting Blade Turbine, low speed flows, linkage effect, fixed blades turbine.

1- Introduction

Utilization of electrical energy is the key to economic growth and improvement in living standards. Rural electrification in developing countries remains a main challenge as is indicated by the 2030 united nations sustainable development goals [1]. The importance of reducing greenhouse gas emissions, depletion of fossil fuel sources, adverse effect of fossil

fuels on the climate and their costs rising, population growth and electrical demand drives research on sustainable energy resources and investigation of more efficient technologies [2-6]. Hydropower, mainly hydrokinetic energy technology, is one of the most vital, reliable and well-distributed renewable energy sources for global electricity generation due to its high density, continuous availability,

predictability and independence weather conditions; it also has a low impact on environmental and human activities [7-9]. Harnessing kinetic energy of flowing water especially is advantageous in regions with numerous riverine resources where dam construction is infeasible or ecologically sensitive [10]. Furthermore, it has the highest global electrical output capacity compared to other renewable sources such as solar, wind, biomass and geothermal energy [11, 12]. Hydropower turbines are one of the most commonly-used technologies extract hydrokinetic energy, in which the turbine blades turn the generator to produce electricity. Differing in their alignments of the turbine axes with respect to the water flow, horizontal axis turbines (HAT) and vertical axis turbines (VAT) are core components of hydrokinetic devices [13-15]. Until now, there has been no consensus on whether the VAT or HAT is the best choice for using river/marine flow energy. However, the VAT appears to have more advantages compared with the HAT in several aspects [4, 6, 17]. The VAT can capture an incoming water flow from any direction and therefore does not need a yaw mechanism, while the HAT does require a yaw mechanism. Also, the VAT is quieter in operation, has reduced mechanical complexity, low cost, simple fabrication and is easy to mount on different ducts [18-22]. Likewise, the VAT is more appropriate than the HAT for lowspeed. In the VAT category, the Savonius turbine is a drag-type rotor and is very commonly applied in regions with lowspeed flows [12, 14, 20,23].

The optimum flow speed for ideal turbine operation is at least 2 m/s [24], while the average flow speed in many locations is 1 m/s [12, 23, 25]. Conventional flow

turbines, which include Darrieus, H-Darrieus and Gorlov turbines, depend very much on the velocity of the flow and thus must operate in a high-speed flow. Hence, the use of conventional flow turbines is not a feasible solution for generating electricity from a low-speed flow.

Numerical methods have been applied in a vast number of scientific studies to determine the efficiency and reliability of a system before designing and actual construction. Because of the savings in time, power of visualization, cost-effectiveness, ease and accuracy provided by simulations, numerical studies are extensively implemented to analyze the flow outline around the blades of a turbine. Computational fluid dynamics (CFD) is a useful numerical method that is extensively employed to analyze turbine performance and solve fluid flow problems.

In the interest of encouraging sustainable energy solutions to attain energy security with a diminished carbon footprint, several studies, both numerical and experimental, have been conducted to develop diverse aspects of the vertical axis turbine (VAT). Quaranta and Davies [25], investigated materials innovative for hydropower application and offered significant information on their performance, benefits and drawbacks [25]. Mat Yazik et al. [7] conducted a numerical study to show the influence of blade angle, water flow velocity, surface roughness and blade material on the performance of a static Savonius hydrokinetic turbine. The simulations revealed that the optimum position for the maximum static torque coefficient, C st=0.30 was at 15° with respect to the fluid flow. Increasing the flow velocity improved the turbine static torque due to an increase in the kinetic energy but increasing the surface roughness has decline effects on the static torque coefficient and decreasing the overall turbine performance [7]. Wong et al. [26] conducted experimental work investigate numerical to the aerodynamic effects of a flat plate deflector on the performance of a vertical axis turbine. The results showed a maximum power coefficient of 33% and that the performance of the turbine was highly dependent on the position of the flat plate deflector. Additionally, the deflector was able to induce a 25% higher velocity compared to the oncoming flow [26]. A numerical investigation was performed by [14], to study Elbertan et al performance of a ducted nozzle Savonius water turbine compared with conventional Savonius turbine. They found that the flow speed was increased by the modified ducted system. The maximum value of the power coefficient was reported to be 0.25 at a tip speed ratio (TSR) of 0.73. The performance of the modified system was enhanced by approximately 78% in comparison with the conventional system. Paniagua. Garsia et al. [23], Studied the effect of blade shape modification Savonius turbine on CFD performance using evaluations, Artificial Neural Network training and Genetic Algorithm optimization. Their finding displayed that the new blade shape improved performance by 8.3% over conventional design. Various studies have focused on optimizing blade shape, implementing endplates and deflectors to improve the turbine performance [27-33]. Ferrari et al. [34], conducted unsteady twodimensional and three-dimensional simulations using a k-ω SST turbulence model to characterize the performance of a Savonius turbine. The results showed a maximum power coefficient of 0.202 at a

TSR of 0.8 for a turbine with an aspect ratio of 1.1. A simulation has been made by Kumar and Saini [35], to analyze a modified Savonius turbine at a flow speed of 2 m/s, which determined a Cpmax of 0.42 for a blade arc angle of 150° and a blade shape factor of 0.6, corresponding to a TSR of 0.9. Alfaro-Ayala et al. [36], applied a numerical study using mesh method dynamic (DMM) to investigate the blade pressure and aerodynamic characteristics for different positions and angular various wind velocities. A numerical analysis was conducted by Hassanzadeh et al. [37], to examine the performance of a new turbine design using folding buckets. This study obtained a Cpmax of 0.321 for a TSR of 0.9, which indicated an improvement of approximately 52% in performance compared conventional design. Numerical investigation of a Darrieus wind turbine with slotted airfoil blades and its comparison with a baseline turbine has been conducted by Mohamed et al. [38], who found that the slotted turbine has a maximum torque coefficient of 0.15 and a maximum power coefficient of 0.3 at a low TSR of 2, approximately three times those of the baseline turbine at same TSR of 2. Also, results showed that the power coefficient of the slotted turbine notably decreased at high TSR and flow separation past the slotted airfoil was delayed at an attack angle of 20°. The performance of a helical Savonius turbine was studied numerically and experimentally, and its results were compared with a two-stage turbine Savonius under the same conditions. The obtained results show that the helical Savonius turbine generates stable torque and a higher power coefficient in comparison with the twostage Savonius turbine [39]. Saad et al.

[40], have conducted a three-dimensional numerical analysis using the URANS equation in conjunction with a k-ω SST turbulence model to determine the optimal design of a twisted-bladed Savonius turbine with a high self-starting capability and the best performance. The effects of different design parameters, as well as overlap ratio, twist angle, endplates size ratio and wind velocity, are investigated. Results indicated that the Savonius turbine with an overlap ratio of zero, a twist angle of 45° and an endplates size ratio of 1.1 achieved the maximum performance. In addition, it was shown that wind speed increases acted to enhance the power coefficient. Subsequently, the optimal configuration attained a high self-starting capability. It is noteworthy experimental work validated the numerical results. The performance of rotors with three cross-sections, namely classic, batchtype and elliptical, was numerically studied by Kacprzak et al. [41] and Frikha et al. [42], conducted numerical simulations in conjunction with standard k–ε and experimental validation to investigate the effect of multi-stage on the efficiency of a Savonius turbine and indicated that a fivestage turbine has a maximum power coefficient of 0.13 among other types of turbines.

The present study aims to analyze the performance parameters of a novel VAT configuration known as a Self-Adjusting Blade Turbine (SABT) using the unsteady RANS equation. in fixed blades turbine operation, the flow impact on the turbine blades is considerable, providing a driving force on one side of the blade turbine (concave side), while on the other side (convex side) there is resistance force from the water. The resultant force causes the turbine to rotate. Therefore. the

performance of the turbine can he improved by minimizing the drag of the water on the convex side of the returning blade. Hence, linkages were applied between blades to allow for adjustment to ensure that the blades rotate around the rotational axis (local axis) and resistance force on the convex side of the blade is minimized. The SABT has two rotational motions when the flow acts on the blades: one is the rotation of the blades around the main axis (shaft of turbine) and the other is the rotation of the bucket around the local axis, which occurs due to the linkage between the blades. In short, as the concave side of the blade (advancing blade) is exposed to the flow, the blade opens fully to maximum effective area and generates maximum force, whilst its counterpart (the returning blade) is fully closed to have minimum effective area and decrease the negative drag force on convex side. The combined effect results in an increase in total torque to the turbine, which will increase power output. Fig. 1 shows the schematic of the SABT.

This work is divided into three parts: the first section discusses the CFD solver setting and numerical procedures to investigate the performance of a fixed-blade turbine (FBT) and SABT at low flow speeds of 0.32 m/s. In the second part, the results from numerical simulation are validated using experimental data. Finally, the performance parameters of the SABT with different arm-length to bucket-diameter ratios (r/d), blade angles (β) and flow velocities were analyzed and reported.

2-Description of the vertical axis turbine

A novel drag base VAT using arms and self-adjusting blades, the SABT, has been designed by Behrouzi et al. [43], as an

alternative to Savonius-based turbines. The appropriate arm length

used in the SABT was found from the results of experiments on three configurations of FBT in which arm length varied. The FBTs were examined to determine the influence of arm length on the performance parameters of the turbine to attain a better configuration in terms of output power. The SABT was constructed based on the FBT results and was examined to investigate the effect of self-adjusting blades on performance. Table 2.1

summarises the tested configurations of the FBT. Consequently, a FBT with an arm length of 270 mm (model 2) which generates maximum torque and power output was chosen as the proper configuration for SABT construction as reported by Behrouzi et al. [43].

The SABT consists of four semi-circular blades, arms, holders, linkages, shaft and bearings; more details can be found in Behrouzi et al. [43].

Table 1: Tested configurations of the fixed blades turbine [43].								
Different configuration	Arm length to bucket diameter ratio (r/d)	Arm length r(m)	Turbine radius R (m) = $r + d$	Turbine diameter D (m)	Bucket diameter d(m)	Turbine height H(m)		
Model 1	1	0.2	0.4	0.8	0.2	1.406		
Model 2	1.35	0.27	0.47	0.94	0.2	1.406		
Model 3	1.7	0.34	0.54	1.08	0.2	1.406		

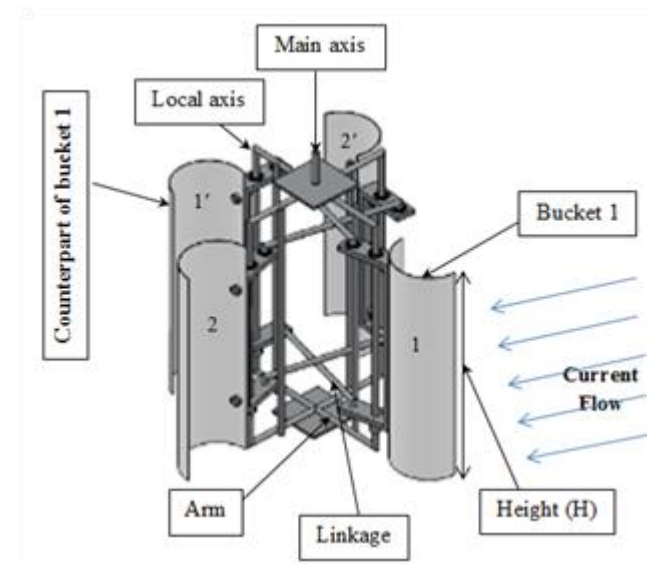


Fig. 1 Schematic representation of self-adjusting blades turbine, including: arms, linkages, blades, main and local axis.

The SABT has two rotational movements when the water flow acts on the blades: the rotation of the blades around the shaft of the turbine (main axis) and the rotation of the buckets around the local axis, which

happens due to the linkages between the blades. Briefly, as the concave side of the advancing blade is exposed to the water flow, the bucket opens fully to its maximum effective area and generates maximum force, whilst its counterpart the returning blade is fully closed, driven by linkages to have a minimum effective area and reduce the negative drag force on the convex side. The combined effects result in a growth in total torque to the turbine, which will increase output power.

3- CFD simulation

3-1- Simulation method

In the ocean engineering community, the standard methods to investigate a turbine characteristic are experimental and numerical works. Due to the high cost of the experimental method, great efforts have been focused on extending numerical methods. CFD has become a valuable

method to evaluate hydrokinetic turbines, which allows investigation of performance parameters and flow patterns without the necessity for instrumentation. hydrokinetic turbines operate on the same conversion principle irrespective of their area of usage in a river or ocean; a set of detailed variations may be imposed in the form of geometry and operational features. The main performance parameters of a turbine torque, rotating are coefficient and TSR.

In the present work, the performance parameters and flow pattern of FBTs with different arm lengths and the performance characteristics of SABTs with variations in (r/d), β and flow speed are numerically investigated. Fig. 2 shows the arm length, bucket diameter and blade angle. The commercial software ANSYS 16.1, using unsteady Reynolds-averaged Navier-Stokes (RANS) equations based on Finite Volume Method (FVM), was applied to solve the dynamics of three-dimensional models for both FBTs and SABTs. In the dynamic study of turbines, the equations are solved using the iterative method for a transient model. To validate and select a suitable turbulence model, a comparison of torque coefficient experimental results with numerical results using two turbulence models $(k - \varepsilon \text{ and } k - \omega SST)$, which were primarily applied to investigate the turbine performance, is shown in Fig. 3. As the results show, the $k - \omega SST$ turbulence model (second order) is the more reliable turbulence model to continue the research.

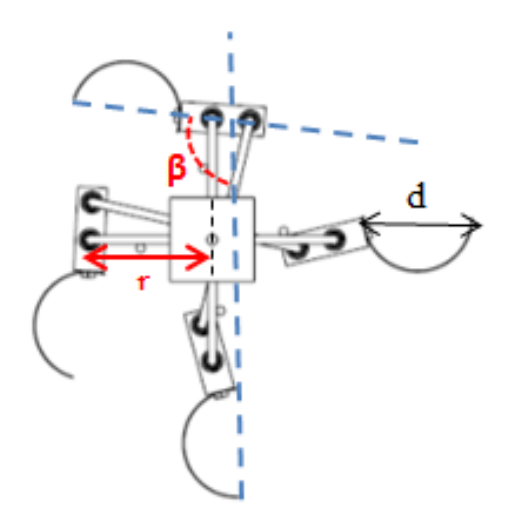


Fig. 2 Schematic representation of arm length, bucket diameter and blade angle.

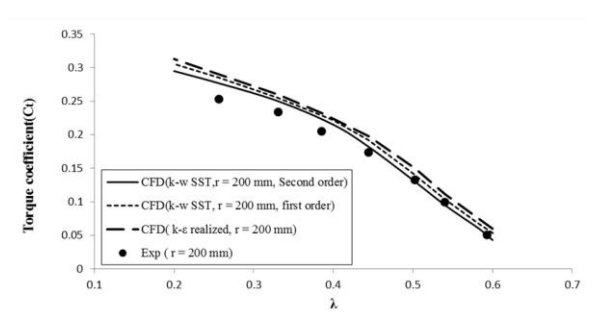


Fig. 3 fixed blades turbine results to validate the CFD result and turbulence model selection.

3-2 Simulation procedure 3-2-1 Fixed-Blade Turbine

The computational domain of the turbine for the dynamic study is separated into a rotating zone and static zone. The two zones are separated by an interface. The rotational domain allows rotating while the stationary domain is fixed. The sizes of the domains are chosen so that the boundaries do not affect the turbine's performance. The circular rotational domain has a diameter of 1.10 D (D = turbine diameter)centred at 6 D from the inlet and sides of the stationary domain. The computational domain of the stationary zone is defined with dimensions of 12 D \times 12 D \times 26 D. geometry, model computational domains and mesh grids have been created using ANSYS-ICEM CFD 16.1. computational domain is shown in Fig. 4. Unstructured mesh was used, which ensures better adaptation to the curved geometry of the turbine. A refined grid was used near the blades in order to correctly predict the flow behaviour in the boundary layer region and get accurate results. The $k - \omega SST$ turbulence model numerically solved using the semi-implicit method for pressure-linked equations (SIMPLE) algorithms for pressure-velocity coupling with second order upwind discretisation. The flow speed of 0.32 m/s was set as the entry and pressure was exerted as the exit of the boundary condition. The sliding mesh model (SMM) was used to solve the rotational motion of the turbine. A no-slip wall condition was considered for the blades. Fig. 5 shows the FBTs tested with different arm lengths.

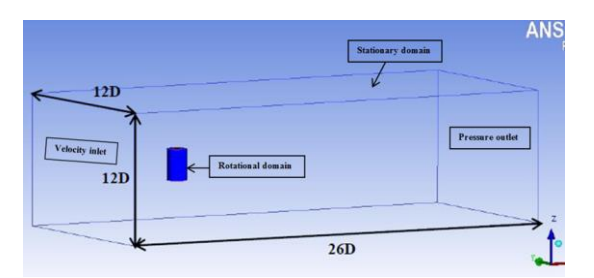
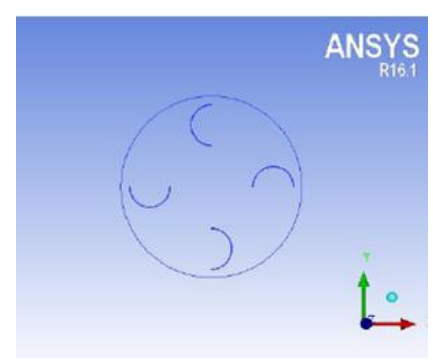
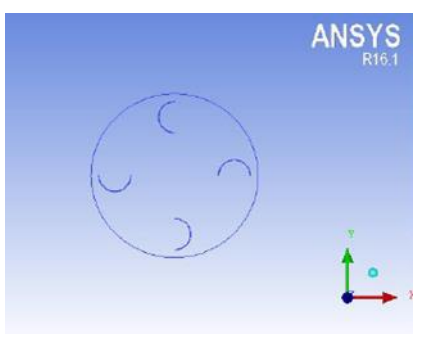


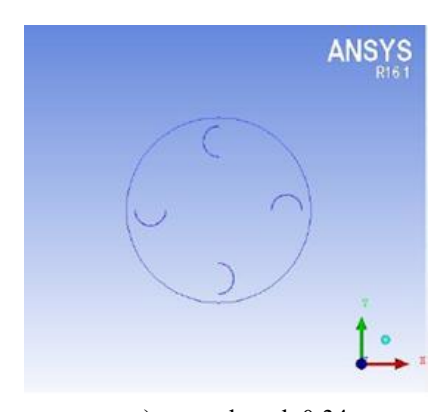
Fig. 4 Computational domain of fixed blades turbine.



a) arm length, 0.2 m



b) arm length, 0.27 m



c) arm length,0.34m

Top view of three configuration of

Fig. 5 Top view of three configuration of fixed blades turbine with different arm length.

3-2-2 Self-adjusting blade turbine

We adapted appropriate settings simulating **SABT** that provide satisfactory accuracy and results acceptable computational creating domains, boundary conditions adequate grids, especially close to the blades. The SolidWorks software was used create the **SABT** design. computational domain size of 12 D \times 12 D × 26 D was considered appropriate for the The computational stationary domain. domains discretised were using unstructured mesh grids created using ANSYS-ICEM CFD 16.1 software. The finest mesh layers were applied near the buckets in order to obtain accurate results. Fig. 6 shows the computational domains and model meshing of the turbine. The k-ω SST eddy viscosity model was used to describe the flow around the turbine. The value of water flow velocity was adopted at the inlet, while the pressure was considered at the outlet of the boundary condition. DMM was applied to solve the rotational movement of buckets around the local axis. DMM was applied to the flow model where the shape of grids changed with time because of movement on the domain boundaries. To confirm rotation of the turbine and each blade around their rotational axes, the main and local axis, respectively, are defined by ANSYS-ICEM CFD. For pressure-velocity coupling, the SIMPLE algorithm was recommended with second-order upwind discretisation. The unsteady pressure-based solver with second-order implicit formulation was applied in this study. The blades were set as a no-slip wall boundary condition.

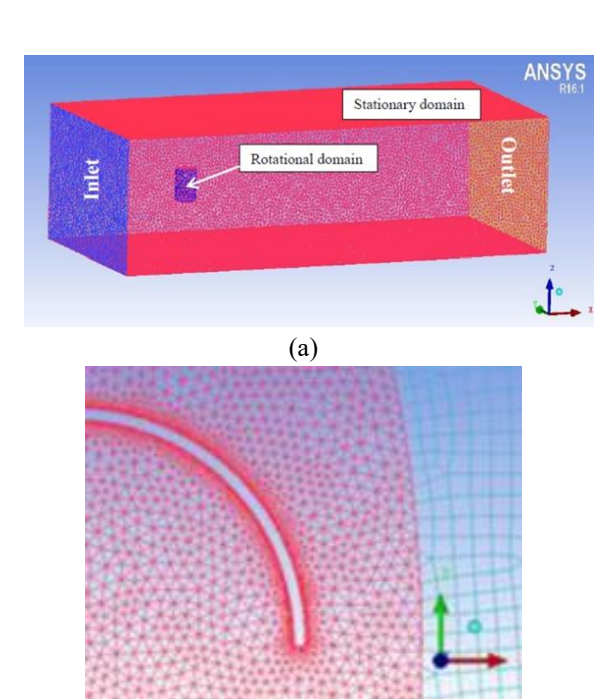


Fig. 6 The computational domains and unstructured mesh grids of turbine. a) overview of the discretized domains, b) the finest grids near the buckets.

(b)

4 Validation study

The CFD simulation of the FBT at three arm lengths and the SABT were validated using the experimental data measured by Behrouzi et al. [43]. The turbine operation can be described using the main parameters: coefficient of torque $(^{C_T})$, coefficient of power $(^{C_p})$ and tip speed ratio (TSR, λ). The dynamic torque coefficient was calculated using equation (1) while equation (2) was used to calculate the power coefficient:

$$C_T = \frac{T}{0.5V_0^2 \rho R A_S} \tag{1}$$

$$C_P = \frac{P_{output}}{0.5V_0^2 \rho R A_s} = C_T \times \lambda$$
 (2)

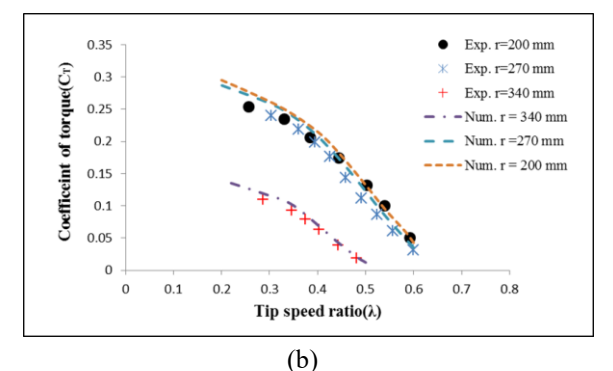
where T and P are the dynamic torque and power of the turbine respectively, $\rho(kg/m^3)$ is the density, $v_0\left(\frac{m}{s}\right)$ is the velocity, R(m) is the maximum radius of the turbine, A_s is the swept area and λ is Tip Speed Raio (TSR), which is defined as:

$$\lambda = \frac{R \omega}{V_0} \tag{3}$$

where ω (rad/s) is the angular velocity. The numerical results of the FBT performance compared with experimental results are plotted in Fig. 7, while the CFD validation of the SABT is shown in Fig. 8.



Experimental setting of fixed blades turbine.



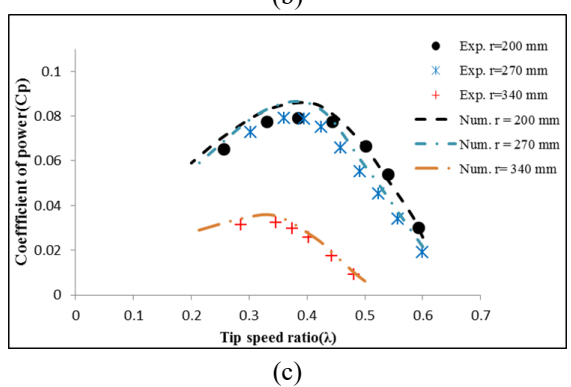
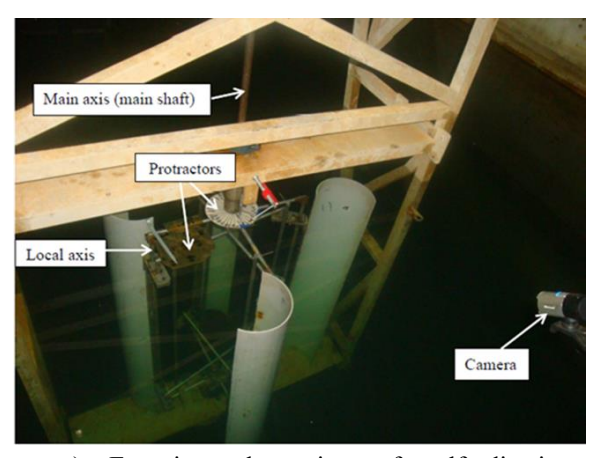
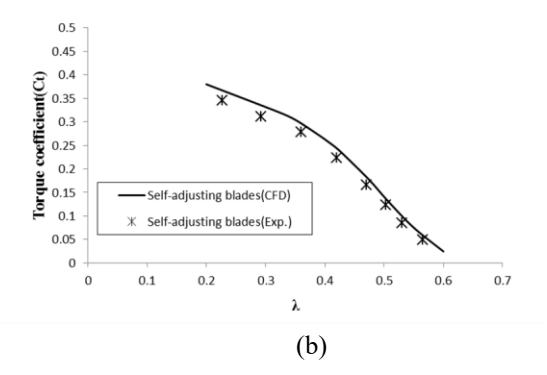


Fig. 7 Comparison of numerical study of fixed blades turbine with experimental works conducted by Behrouzi et al. [43]. a) experimental setting b) coefficient of torque, c) coefficient of power.



a) Experimental setting of self-adjusting blades turbine.



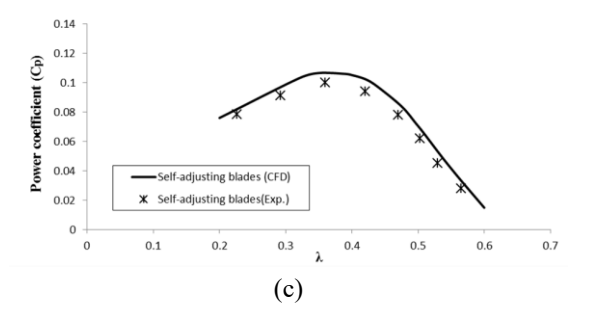


Fig. 8 CFD validation of self-adjusting blades turbine using exprtimetal data conducted by Behrouzi et al. [43]. a) experimental setting b) torque coefficient c) power coefficient.

The simulation and experiments have reasonably similar trends and their results show good agreement with each other. There are a few differences between numerical and experimental results; the value of the numerical simulation is slightly higher than in the experimental results. The difference between experimental and numerical results of fixed blades turbine at maximum values are 8.9%, 6.7% and 8.6% for arm length 200 mm, 270 mm, and 340 mm, respectively. Also, the maximum error percentage of self-adjusting blades turbine is calculated These small differences can be attributed to experimental and numerical error due to some uncertain factors that led to a decrease in the obtained torque value. The holding structure of the turbine model test is one parameter which appeared to cause differences in the results. It caused some loss of torque produced from the turbine shaft. Also, the SABT included movable parts and other factors such as water viscosity, friction in the bearings, pulleys and wiring, etc. These may have introduced extra friction which led to errors between numerical and experimental results.

In sum, despite small differences between numerical and experimental results, there is good agreement between the simulation and experimental results which suggest that the numerical simulations have been validated by experimental tests.

5 Results and discussion

The CFD models were used to analyse and discuss different geometrical parameters of the SABT. This paper presents investigations of the effects of different (r/d) and β parameters, by determining the performance and characteristics of flow of the SABT. The influence of various water flow velocities on the performance of a modified SABT is also examined.

5-1 Variation of arm length to bucket diameter ratio (r/d).

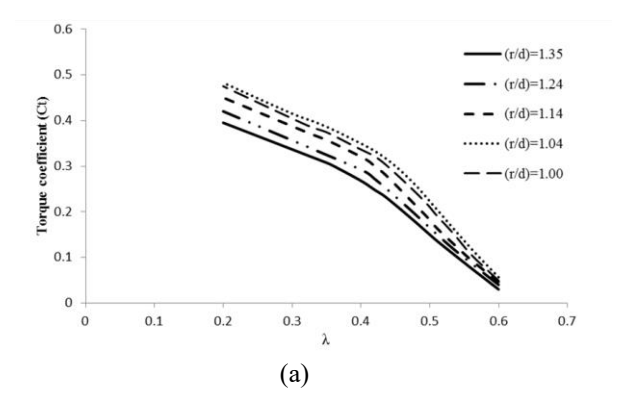
This section reports results from the numerical studies on the influence of several (r/d) values on the performance of SABTs with a constant turbine radius (R= 470 mm). Table 5.1 shows the five different (r/d) values for the SABT numerical simulation.

Table 2: Configurations of buckets and arm in self-adjusting blades turbine.

dajusting blades taronie.							
G 11:1	Arm length	Bucket diameter	Arm length to bucket				
Conditions	r (mm)	d (mm)	diameter				
			ratio (r/d)				
Case1	270	200	1.35				
Case2	260	210	1.24				
Case3	250	220	1.14				
Case4	240	230	1.04				
Case5	235	235	1.00				

In Figs. 9(a) and 9(b), the obtained values for the coefficients of torque and power versus different TSR for five cases are shown.

From Fig. 9, it can be seen that the turbine had the best performance for the (r/d) value of 1.04, with a maximum power coefficient value of 0.14 at TSR=0.42.



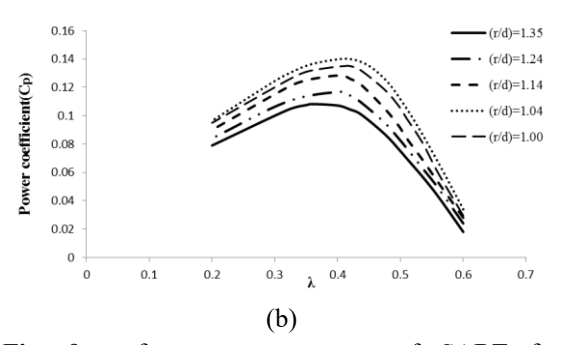


Fig. 9 performance parameters of SABT for different arm length and bucket diameter ratio (r/d), a) torque coefficient, b) power coefficient.

The torque and power coefficients grew while values of (r/d) decreased until they reached 1.04; afterwards, the reduction in the (r/d) ratio caused a decrease in the torque and power coefficients. As the blades play an important role in turbine operation and they are exposed to water flows more than other parts, the above results occurred because the bucket area increased with decreasing (r/d), which means more interaction between the water flow and buckets occurred and led to an increase in the resultant force acting on the blades. In case 5, the value of the maximum power coefficient decreased due to the increase in interference effects between blades and other accessories which caused the loss of positive drag from water acting on the concave side of the advancing blades.

In Fig. 10, the velocity streamlines for the best condition of the turbine performance are shown. The flow velocity streamlines

around the convex side of buckets increased. The hydrodynamic pressure on the convex side of the buckets decreased due to a flow velocity increase that generated the lifting force which added power to the turbine. In the case of the SABT with (r/d) = 1.04, the flow velocity increase on the convex side of the buckets was greater than in other cases, which led an increase in the lifting force component and increased the resultant force and performance of the turbine. The velocity streamlines for the turbine buckets with extreme values of (r/d) are shown in Fig. 10(b). It can be seen that the decreased bucket area led to diminished water pressure on the concave side of the advancing blades. which caused resultant force and performance to decrease at (r/d) = 1.35.

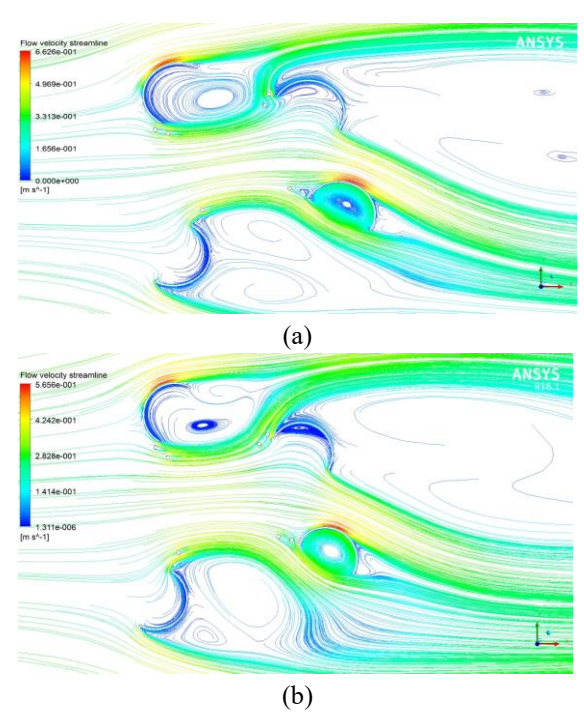
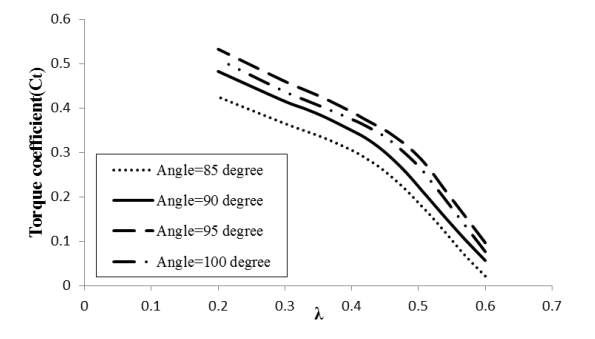


Fig. 10 Velocity stream line of self-adjusting blades turbine (a) r/d=1.04 (b) r/d=1.35.

5-2 Variation of blade angle

The blade angle (β) is specified as the angle between the chord of one bucket and its opposite counterpart, as shown in Fig. 11. The linkages connected a bucket with

its opposite counterpart to adjust β and to ensure that a bucket moved in a direction opposite to its counterpart. Hence, a change in linkage length can change the β . For the conventional SABT constructed by Behrouzi et al. [43], β was defined as 90° through the installation of linkages. Experimental tests indicated that as the turbine rotated, the advancing blade fully opened to a maximum effective area at the same time that its counterpart closed to reduce the resistance force with a β of 90°, except at the beginning of each quarterrevolution at which the full opening of the blade is delayed. The advancing blades fully opened at the turbine angle of 30° to 38° for each quarter-revolution reported by Behrouzi et al. [43]. Hence, we needed to modify the turbine operation to solve the abovementioned problem using different β .



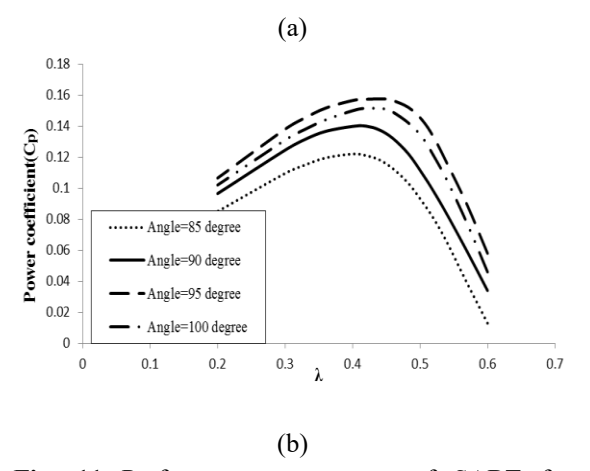


Fig. 11 Performance parameters of SABT for different blade angle (β) , a) torque coefficient, b) power coefficient.

Numerical simulation was conducted on the SABT turbine with an (r/d) of 1.04 while varying β . The β values studied are 85°, 90°, 95° and 100°. Fig. 11 shows the variation of torque and power coefficients for different β. A turbine with a β of 95° has a higher power coefficient compared to turbines with other β values of 85°, 90° and 100°, as can be seen in Fig. 11(b). The maximum power coefficient value for a turbine with a β of 95° is approximately 0.16 with corresponding $\lambda = 0.45$. It was observed that for a \beta of 95°, at the beginning of each quarter the advancing blade fully opened at the turbine angle lower than 30°, which led to greater water pressure and increased the torque and performance of the turbine, while in a turbine with a blade angle of 100°, the immediate opening of the advancing blade caused an increase in negative drag of its counterpart (returning blade), consequently reducing the total torque and performance of this turbine compared to one with a 95° blade angle. Also, for a turbine with a β of 85°, the full opening of the advancing blade happened with more delaying compared to other β values of 90°, 95° and 100°, which imposed extra suction and circulation behind the blades and led to a reduction in turbine performance.

Fig. 12 shows the velocity vector of the SABT for β of 95°. The SABT with a β of 95° captured more water pressure on the concave side of the advancing blades.

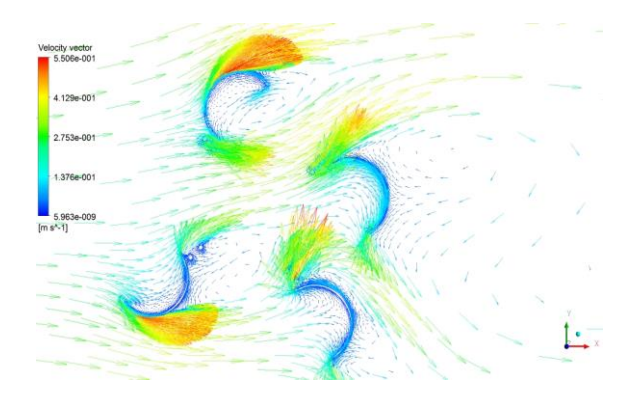


Fig. 12 Velocity vector of self-adjusting blades turbine for blade angle 95°

The velocity streamlines of the SABT with a β of 85° are depicted in Fig. 13. There was more circulation behind the closed blades of the SABT at the β of 85°, which caused the turbine performance to decline.

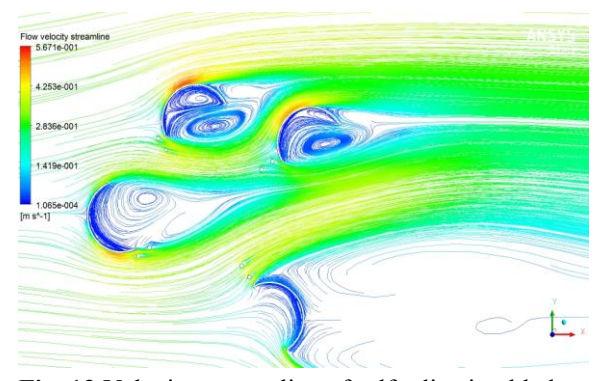


Fig. 13 Velocity stream line of self-adjusting blades turbine for blade angle 85°.

5-3 Variation of flow velocity

The influence of different flow velocities was investigated for a modified SABT with r/d=1.04, and a β of 95°. Fig. 14 illustrates the variation of torque and power coefficients for flow speeds of 0.17 m/s, 0.32 m/s and 0.64 m/s.

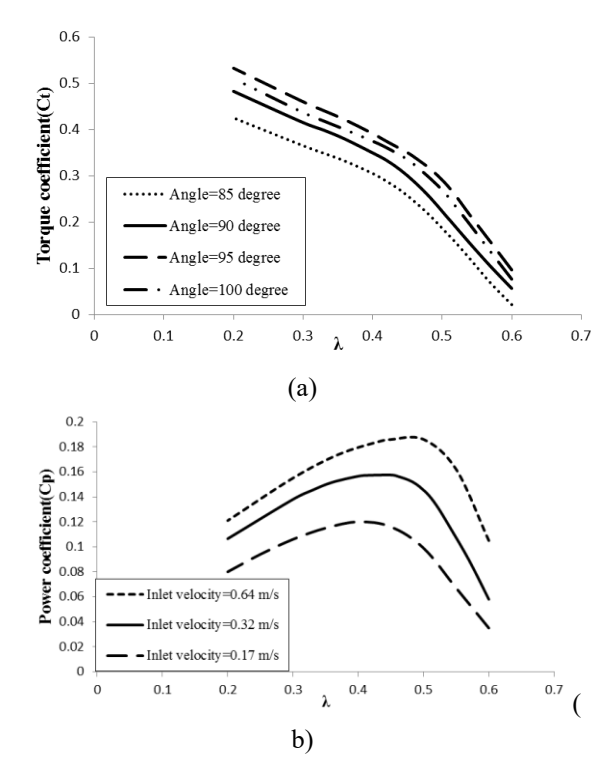


Fig. 14 performance parameters of SABT for different flow velocity, a) torque coefficient, b) power coefficient.

The coefficients of power and torque increased as the flow velocity increased from 0.17 m/s to 0.64 m/s as depicted in Fig. 14. In this figure, it can be seen that the TSR range for the maximum power coefficient lies between 0.4 and 0.5. It is noteworthy that the inlet flow velocity is a main factor which can affect turbine operation and flow characteristics such as flow separation and boundary layer formation around the turbine. A flow velocity increase caused an increase in the rotational rate of the turbine and delayed separation around the turbine blades, which led to negative drag reduction and increased the resultant force. As a result, the turbine performance increased with increasing inflow velocity.

6- Conclusion

In this article, a CFD study was conducted in order to evaluate the performance of a novel design of VACT, called a selfadjusting blade turbine, for ocean flow applications, especially in remote areas with low-speed flows. The unsteady RANS equation, based on finite volume methods using SIMPLE algorithms with secondupwind discretisation and $k - \omega$ SST turbulence model, was applied to obtain accurate results. The finest mesh volume grids were used close to the blades in order to obtain reliable results. The numerical results were validated using experimental data. Furthermore, the torque and power coefficients of SABTs were studied using geometric parameters by varying the arm length to bucket ratios, blade angles and operating conditions such as different flow speeds. The detailed streamlines were analysed and reported. The results support the conclusions below:

- 1) This paper showed that the arm length and blade angle have a strong effect on turbine performance. The maximum power coefficient of the modified SABT was 0.16 with a corresponding $\lambda = 0.45$ at a flow velocity of 0.32 m/s.
- 2) Among turbine models using different (r/d) values with a constant turbine radius, the maximum performance occurred in a turbine with an (r/d) value of 1.04, due to greater interaction between the inflow flow and buckets.
- 3) The operation of the SABT turbine was modified using a blade angle of 95°, which solved the problem associated with the full opening of the advancing blade at the beginning of each quarter.
- 4) Increasing inflow velocity led to increases in the torque and power coefficients of the turbine due to rotational velocity increases and flow

separation delays around the turbine blades.

References

- [1] Silinto, B. F., van der Laag Yamu, C., Zuidema, C., & Faaij, A. P. (2025). Hybrid renewable energy systems for rural electrification in developing countries: A review on energy system models and spatial explicit modelling tools. *Renewable and Sustainable Energy Reviews*, 207, 114916.
- [2] Behera, U. S., Sangwai, J. S., & Byun, H. S. (2025). A comprehensive review on the recent advances in applications of nanofluids for effective utilization of renewable energy. *Renewable and Sustainable Energy Reviews*, 207, 114901.
- [3] Nassar, Y. F., El-Khozondar, H. J., & Fakher, M. A. (2025). The role of hybrid renewable energy systems in covering power shortages in public electricity grid: An economic, environmental and technical optimization analysis. *Journal of Energy Storage*, 108, 115224.
- [4] Liu, S., Zhang, L., Lu, J., Zhang, X., Wang, K., Gan, Z., ... & Wang, H. (2025). Advances in urban wind resource development and wind energy harvesters. *Renewable and Sustainable Energy Reviews*, 207, 114943.
- [5] Avarand, S., & Pirmoradian, M. (2016). Solar tracking system with momentary tracking based on operational amplifiers in order to be used in photovoltaic panels for following the sun. *Bulletin de la Société Royale des Sciences de Liège*, 85(9).
- [6] Deng, Q., Alvarado, R., Toledo, E., & Caraguay, L. (2020). Greenhouse gas emissions, non-renewable energy consumption, and output in South America: the role of the productive structure. *Environmental Science* and Pollution Research, 27(13), 14477-14491.
- [7] Yazik, M. H. M., Zawawi, M. H., Ahmed, A. N., Sidek, L. M., Basri, H., & Ismail, F. (2024). One-way fluid structure interaction analysis of a static savonius hydrokinetic turbine under different velocity and surface roughness with different blade materials. *Ocean Engineering*, 291, 116373.
- [8] Williams, G.G., and Jain, P. (2011). Renewable energy strategies. Sustain: a Journal of Environmental and Sustainability issues, the

- Kentucky Institute for the Environment and Sustainable Development. 23, 29–42.
- [9] Elghali, S. B., Benbouzid, M. E. H., & Charpentier, J. F. (2007, May). Marine tidal current electric power generation technology: State of the art and current status. In 2007 IEEE International Electric Machines & Drives Conference (Vol. 2, pp. 1407-1412). IEEE.
- [10] Ridgill, M., Lewis, M. J., Robins, P. E., Patil, S. D., & Neill, S. P. (2022). Hydrokinetic energy conversion: A global riverine perspective. *Journal of Renewable and Sustainable Energy*, 14(4).
- [11] Ember, 2022. Yearly electricity data. https://ember-limate.org/app/uploads/2022 /07/yearly full release long format.csv.
- [12] Salleh, M. B., Kamaruddin, N. M., & Mohamed-Kassim, Z. (2019). Savonius hydrokinetic turbines for a sustainable riverbased energy extraction: A review of the technology and potential applications in Malaysia. Sustainable energy technologies and assessments, 36, 100554.
- [13] Khan, M. J., Bhuyan, G., Iqbal, M. T., & Quaicoe, J. E. (2009). Hydrokinetic energy conversion systems and assessment of horizontal and vertical axis turbines for river and tidal applications: A technology status review. *Applied energy*, 86(10), 1823-1835.
- [14] Elbatran, A. H., Ahmed, Y. M., & Shehata, A. S. (2017). Performance study of ducted nozzle Savonius water turbine, comparison with conventional Savonius turbine. *Energy*, 134, 566-584.
- [15] Saini, G., & Saini, R. P. (2019). A review on technology, configurations, and performance of cross-flow hydrokinetic turbines. *International Journal of Energy Research*, 43(13), 6639-6679.
- [16] Eriksson, S., Bernhoff, H., & Leijon, M. (2008). Evaluation of different turbine concepts for wind power. renewable and sustainable energy reviews, 12(5), 1419-1434.
- [17] Kirke, B. (2020). Hydrokinetic turbines for moderate sized rivers. *Energy for Sustainable Development*, 58, 182-195.
- [18] Khan, R., & Kumar, A. (2024). Performance enhancement of hydrokinetic turbine using augmentation techniques: a review. *International Journal of Green Energy*, 21(7), 1667-1694.

- [19] Aly, H. A.A. (2016). Micro Hydraulic Turbine for Power Generation in Micro Scale Channels. PhD thesis. Universiti Teknologi Malaysia, Skudai.
- [20] Suprayogi, D. T. (2010). Savonius rotor vertical axis marine current turbine for renewable energy application (Doctoral dissertation, Universiti Teknologi Malaysia).
- [21] Zhou, H. (2012). Maximum power point tracking control of hydrokinetic turbine and low-speed high-thrust permanent magnet generator design.
- [22] Hofemann, C., Ferreira, C. S., Dixon, K., Van Bussel, G., Van Kuik, G., & Scarano, F. (2008). 3D Stereo PIV study of tip vortex evolution on a VAWT. European Wind Energy Association EWEA, 1-8.
- [23] Paniagua-García, E., Taborda, E., Nieto-Londoño, C., Sierra-Pérez, J., Vásquez, R. E., & Perafán-López, J. C. (2025). A meta-model based cross-sectional shape of a Savonius hydrokinetic turbine for sustainable power generation in remote rural areas. *Renewable Energy*, 244, 122647.
- [24] Hassan, H. F., El-Shafie, A., & Karim, O. A. (2012). Tidal current turbines glance at the past and look into future prospects in Malaysia. *Renewable and Sustainable Energy Reviews*, 16(8), 5707-5717.
- [25] Quaranta, E., & Davies, P. (2022). Emerging and innovative materials for hydropower engineering applications: Turbines, bearings, sealing, dams and waterways, and ocean power. *Engineering*, 8, 148-158.
- [26] Wong, K. H., Chong, W. T., Sukiman, N. L., Shiah, Y. C., Poh, S. C., Sopian, K., & Wang, W. C. (2018). Experimental and simulation investigation into the effects of a flat plate deflector on vertical axis wind turbine. *Energy Conversion and Management*, 160, 109-125.
- [27] Shanegowda, T. G., Shashikumar, C. M., Gumtapure, V., & Madav, V. (2024). Comprehensive analysis of blade geometry effects on Savonius hydrokinetic turbine efficiency: Pathways to clean energy. *Energy Conversion and Management: X*, 24, 100762.
- [28] Kadam, A. R., & Parida, R. K. (2024). Numerical studies on the performance of Savonius turbines for hydropower application by varying the frontal cross-sectional area. *Ocean Engineering*, 306, 117922.
- [29] Zamani, M., Nazari, S., Moshizi, S. A., & Maghrebi, M. J. (2016). Three dimensional

- simulation of J-shaped Darrieus vertical axis wind turbine. *Energy*, *116*, 1243-1255.
- [30] Kumar, R., & Kumar, A. (2024). Optimization of slot parameters for performance enhancement of slotted Savonius hydrokinetic turbine using Taguchi analysis. *Renewable Energy*, 237, 121608.
- [31] Wang, X. H., Foo, J. S. Y., Fazlizan, A., Chong, W. T., & Wong, K. H. (2024). Effects of endplate designs on the performance of Savonius vertical axis wind turbine. *Energy*, *310*, 133205.
- [32] Salleh, M. B., & Kamaruddin, N. M. (2025). Power performance and flow structure analysis of a deflector-augmented savonius hydrokinetic turbine under variable flow speeds. *Ocean Engineering*, 325, 120789.
- [33] Guo, F., Song, B., Mao, Z., & Tian, W. (2020). Experimental and numerical validation of the influence on Savonius turbine caused by rear deflector. *Energy*, *196*, 117132.
- [34] Ferrari, G., Federici, D., Schito, P., Inzoli, F., & Mereu, R. (2017). CFD study of Savonius wind turbine: 3D model validation and parametric analysis. *Renewable energy*, 105, 722-734.
- [35] Kumar, A., & Saini, R. P. (2017). Performance analysis of a single stage modified Savonius hydrokinetic turbine having twisted blades. *Renewable Energy*, 113, 461-478.
- [36] J. Arturo Alfaro-Ayala, A. Gallegos-Mu~noz, J. Manuel Belman-Flores,(2011). Experimental and Numerical Analysis of a Vertical Axial Wind Turbine Applying the Dynamic Mesh Method.
- [37] Hassanzadeh, R., bin Yaakob, O., Taheri, M. M., Hosseinzadeh, M., & Ahmed, Y. M. (2018). An innovative configuration for new marine current turbine. *Renewable Energy*, 120, 413-422.
- [38] Mohamed, O. S., Ibrahim, A. A., Etman, A. K., Abdelfatah, A. A., & Elbaz, A. M. (2020). Numerical investigation of Darrieus wind turbine with slotted airfoil blades. *Energy Conversion and Management: X*, 5, 100026.
- [39] Kothe, L. B., Möller, S. V., & Petry, A. P. (2020). Numerical and experimental study of a helical Savonius wind turbine and a comparison with a two-stage Savonius turbine. *Renewable Energy*, 148, 627-638.
- [40] Saad, A. S., El-Sharkawy, I. I., Ookawara, S., & Ahmed, M. (2020). Performance enhancement of twisted-bladed Savonius

- vertical axis wind turbines. *Energy Conversion and Management*, 209, 112673.
- [41] Kacprzak, K., Liskiewicz, G., & Sobczak, K. (2013). Numerical investigation of conventional and modified Savonius wind turbines. *Renewable energy*, 60, 578-585.
- [42] Frikha, S., Driss, Z., Ayadi, E., Masmoudi, Z., & Abid, M. S. (2016). Numerical and experimental characterization of multi-stage Savonius rotors. *Energy*, 114, 382-404.
- [43] Behrouzi, F., Nakisa, M., Maimun, A., Ahmed, Y. M., & Souf-Aljen, A. S. (2019). Performance investigation of self-adjusting blades turbine through experimental study. *Energy conversion and management*, 181, 178-188.